Evidence for collective behavior in ^{128}Ce from lifetime measurements

J. C. Wells
Tennessee Technological University, Cookeville, Tennessee 38505
and Oak Ridge National Laboratory, Oak Ridge, Tennessee 37831

N. R. Johnson, J. Hattula,* M. P. Fewell,† D. R. Haenni,‡ I. Y. Lee, F. K. McGowan, and J. W. Johnson
Oak Ridge National Laboratory, Oak Ridge, Tennessee 37831

L. L. Riedinger
University of Tennessee, Knoxville, Tennessee 37916
and Oak Ridge National Laboratory, Oak Ridge, Tennessee 37831

(Received 29 May 1984)

Lifetimes in the yrast sequence of ^{128}Ce have been measured following the reaction ^{92}Zr(^{40}Ar, 4n) induced by 159-MeV ^{40}Ar ions. A Doppler-shift recoil-distance device was utilized inside a large NaI detector where the latter provided total γ-ray decay energy selection for these measurements. The $B(E2)$ values deduced for the 2^+ through 14^+ states indicate that in the ground band ^{128}Ce conforms much more closely to rigid-rotor behavior than do the heavier cerium isotopes, and that in the s band the shape parameters remain in the collective sector $-60° < \gamma < 0°$, as predicted by cranked self-consistent theory.

I. INTRODUCTION

In earlier studies on ^{130,132,134}Ce, Husar *et al.*[1] and Nolan *et al.*[2,3] obtained both energy-level spacings and lifetime results which indicated increased collective behavior with decreasing neutron number. In addition, they found that in each of these nuclei the $B(E2)$ value of the $10^+ \rightarrow 8^+$ transition, which corresponds to the onset of backbending, was noticeably reduced when compared with the predicted rotational value. This latter effect was greatest in ^{134}Ce (96% reduction) and least in ^{130}Ce (50% reduction). These findings prompted us to carry out lifetime measurements on ^{128}Ce to see if this pattern of increasing collectivity continues, and to further study the behavior of $B(E2)$ values in the vicinity of the backbend.

To establish the prominent features of the ^{128}Ce level scheme, Carvalho *et al.*[4,5] first carried out general spectroscopy measurements using the reaction ^{112}Cd(^{20}Ne,4n) ^{128}Ce. They determined the yrast sequence up to $I = 24^+$ and assigned with less certainty two partially developed sidebands. The level scheme shown in Fig. 1 summarizes these results (from Refs. 4 and 5). Angular distribution results[4,5] showed that the yrast sequence in this scheme consists of stretched-$E2$ transitions, as does sideband 1. However, it was not possible to establish the multipolarity for the transitions between sideband 1 and the ground band or for the transitions in sideband 2.

II. EXPERIMENTAL PROCEDURE

In the present measurements, lifetimes of the yrast states of ^{128}Ce were investigated by the Doppler-shift recoil-distance technique. The recoil-distance device, shown in Fig. 2, incorporates stretched foils for the target and stopper and three differential thread adjustments for their parallel alignment. Parallelism is achieved by first reflecting a laser beam either off of the target or, if the target is a poor reflector, off of a nickel foil stretched over the "target stretcher cone." With the target mounted, the

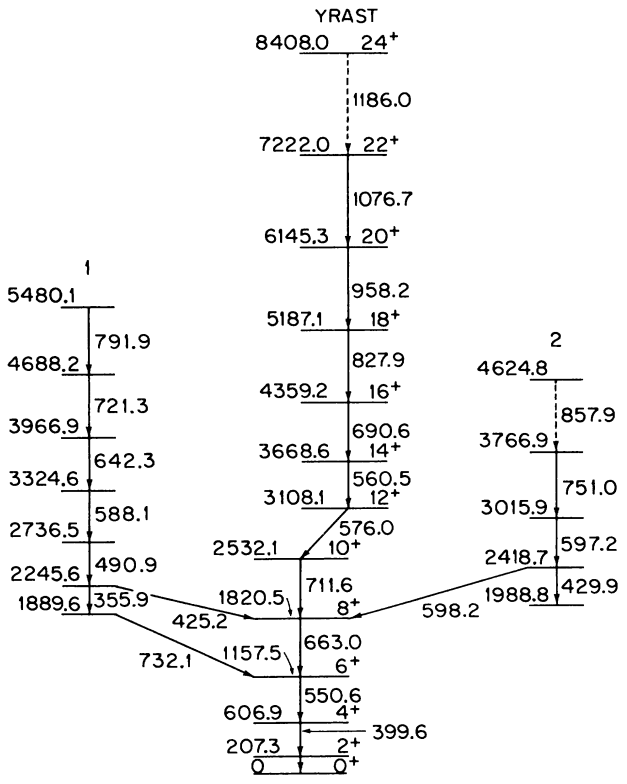

FIG. 1. Level scheme of ^{128}Ce determined from the reaction ^{112}Cd(^{20}Ne, 4n)^{128}Ce by Carvalho *et al.* (Refs. 4 and 5).

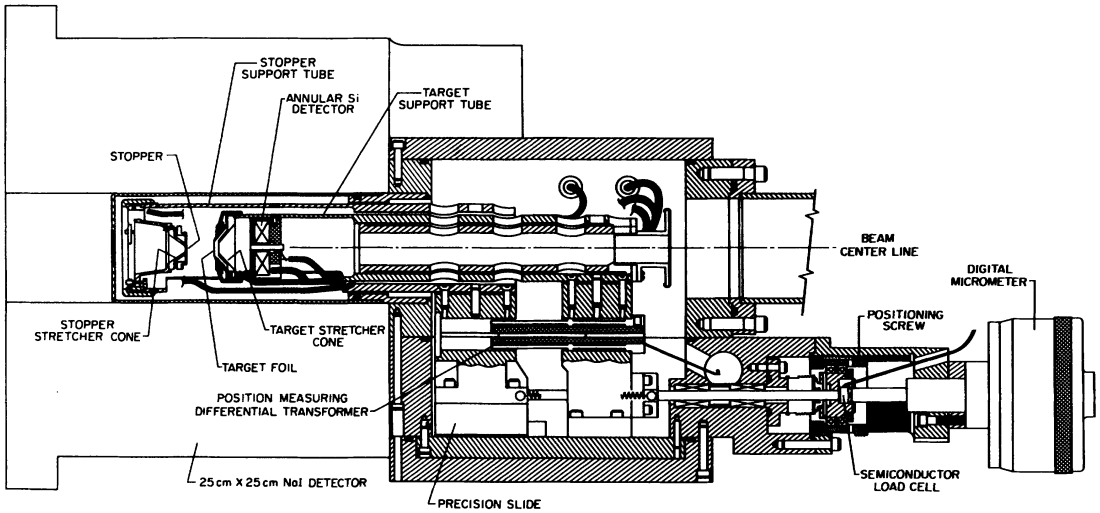

FIG. 2. A schematic representation of the Doppler-shift recoil-distance device and the total-energy spectrometer used in the present measurements.

assembly containing the "stopper" is inserted and the laser beam is reflected off the nickel backing of the lead stopper. Adjustments of the differential screws necessary to bring the stopper into parallel alignment with the target are then performed. Target-stopper separations were determined by a position-measuring differential transformer, a digital readout micrometer having a piezoelectric load cell for positioning, and by pulser-capicitance measurements at small distances. The apparatus fits inside the annular opening of a 25-cm×25-cm NaI total-energy detector. Additional details on the Doppler-shift device are given in Ref. 6.

To provide a greater recoil velocity for the lifetime measurements, we used a 159-MeV ^{40}Ar beam from the Oak Ridge Isochronous Cyclotron to induce the ^{92}Zr(^{40}Ar,4n)^{128}Ce reaction. In producing very neutron deficient nuclei such as ^{128}Ce, it is necessary to contend with a large number of reaction channels, with many of these arising from charged particle emission. Since the experimental data were stored in list mode on magnetic tape as three-parameter events (γ-ray energy, total γ-ray decay energy, and timing information), it was possible to achieve some selectivity of the desired reaction channel. This was done in post-experiment analyses by requiring a coincidence between γ rays intercepting the Ge detector and an appropriately gated region of the total-energy spectrum. Figure 3 illustrates the advantages of this technique. Spectrum (a) is in coincidence with the highest energy region of the total energy, and (b), (c), and (d) result from successively lower-energy regions. We see that spectra (a) and (b) are dominated by ^{126}Ba(α2n), ^{129}La(p2n), and ^{129}Ce(3n), where the particles in parentheses represent those emitted in the respective reactions. Spectrum (c), which was used in the present analysis, contains primarily ^{128}Ce(4n), and spectrum (d), in coincidence with the lowest total energy, shows ^{128}Ba(2p2n) and ^{127}La(p4n).

Shifted and unshifted γ-ray energies and intensities were measured with a large volume Ge(Li) detector for ten recoil flight distances, ranging from 9.3 μm to 2.03 mm. Figure 4, showing shifted and unshifted γ-ray peaks for the 4^+ through 16^+ states at three of these distances, is presented for illustrative purposes. Gamma-ray intensities were extracted from the spectra by a peak-fitting computer program and were normalized to the total γ-ray intensity in the energy range 1500—2000 keV, a region in which there were no intense discrete γ rays. The recoil

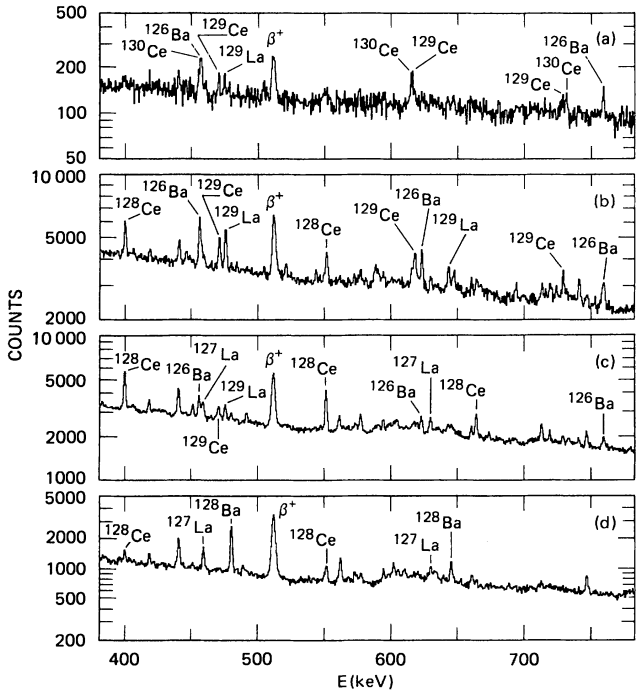

FIG. 3. Gamma-ray spectra resulting from gating on different regions of the total decay energy spectrum following the reactions induced by 159-MeV ^{40}Ar ions on ^{92}Zr. Spectrum (a) is that from the highest cut in total energy, while (b), (c), and (d) result from successively lower-energy cuts. Spectrum (c) is optimum for analysis of ^{128}Ce.

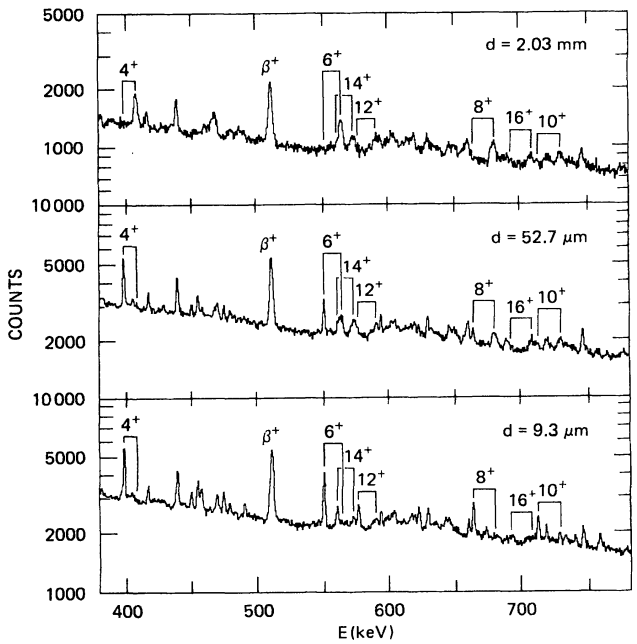

FIG. 4. Gamma-ray spectra showing shifted and unshifted peaks for the 4^+ through 16^+ members of the ^{128}Ce yrast sequence at three of the ten target-stopper separations in the present measurements.

velocity, determined from the energy shifts, was 7.26 ± 0.12 μm/ps, which corresponds to $(0.0242\pm0.0004)C$.

III. DATA ANALYSIS AND RESULTS

The extracted intensities (decay curves) were analyzed with the computer program LIFETIME,[7] which was developed at Oak Ridge National Laboratory (ORNL) from a version supplied by Hans Emling of Gesellschaft für Schwerionenforschung and which incorporates the general-purpose minimization routine MINUIT.[8] The program performs a least-squares fit of shifted and unshifted intensities with initial level populations and transition probabilities being treated as the variable parameters. The shifted and unshifted intensities were fitted separately to determine the best value of the lifetime, rather than fitting the ratio of unshifted to total intensity, as is usually done.

Corrections to the data were made (a) for the change in solid angle as a function of position along the flight path, (b) for the dependence of solid angle on velocity, (c) for the γ-ray line shape of the shifted peak as the recoils are slowing down in the stopper, and (d) for the change in the angular distribution of the γ rays due to the loss of alignment caused by electronic hyperfine interactions during flight. For this last correction, the angular distribution was assumed to have the form

$$W(\theta,t)=1+A_2\exp(-t/\tau_2)P_2(\cos\theta) + A_4\exp(-t/\tau_4)P_4(\cos\theta)\ , \quad (1)$$

where t is the time at which the γ ray is emitted. For the shifted peak correction, the angular distribution was averaged over the flight time, while for the unshifted peak correction, it was evaluated with t equal to the flight time, since the alignment attenuation is assumed to stop when the recoil nucleus enters the stopper. (See discussions in Refs. 9 and 10 for details.) The values used for the relaxation times, $\tau_2=30$ ps and $\tau_4=10$ ps, are based on earlier measurements of nuclei in this region by Ward *et al.*,[11] as well as on studies[12] of the effects on the lifetime values in ^{150}Nd resulting from variations of τ_2 and τ_4.

Data were obtained for the 2^+ through 16^+ states of the yrast sequence. Two-step cascade side feeding was assigned to the 2^+, 6^+, 8^+, 12^+, and 14^+ states. No side feeding was assigned into the 4^+ and 10^+ states because the intensity balances did not require it. We utilized the 16^+ through 24^+ yrast states in the analysis of the lower states by assuming that they are members of a rotational band with constant intrinsic quadrupole moment Q_0 and that their lifetimes are given by the expression

$$\frac{1}{\tau}=1.22E_\lambda^5Q_0^2(I\,2\,0\,0\,|\,I-2\,0)^2\ \text{ps}^{-1}\ , \quad (2)$$

where E_λ is the experimental transition energy and Q_0 is treated as a variable parameter.

The parameters which were varied during the fitting were the following: all of the transition probabilities, the initial populations of the 24^+ state and all side feeding states, and the quadrupole moment Q_0 of the rotational band assumed to feed the 14^+ member. (The best-fit value of Q_0 was 2.1 ± 0.2 e b.) Initial populations of the 2^+ through 22^+ states were fixed at zero. The lifetimes and reduced transition probabilities determined from these measurements are summarized in Table I. In Fig. 5 we show the corrected intensities of the unshifted peaks for ^{128}Ce yrast transitions as a function of the flight time for each target-stopper separation. The solid curve in each case is the fit to the data determined from the program LIFETIME.[7] Although not shown here, the information taken at the longer distance was essential in determining the lifetime of the 2^+ state.

In a compound nucleus reaction, the problems presented by side feeding to a given level can greatly complicate the extraction of a reliable lifetime and the assignment of meaningful error limits. Therefore, we shall present in some detail the procedure used to obtain the best fit to the decay curves and to obtain the best values of the lifetimes in ^{128}Ce. The fitting procedures were carried out in several steps, with the result of a previous step being used as the starting values of the next step. Initially, all levels

TABLE I. Lifetimes and reduced transition probabilities of yrast states of ^{128}Ce.

E_γ (keV)	I^π	τ (ps)	$B(E2)$ (e^2b^2)
207	2^+	427^{+38}_{-34}	0.43 ± 0.04
400	4^+	$11.6^{+2.6}_{-2.0}$	0.68 ± 0.13
551	6^+	$2.9^{+1.9}_{-1.5}$	$0.6^{+0.5}_{-0.2}$
663	8^+	$0.8^{+0.6}_{-0.8}$	$0.8^{+80}_{-0.3}$
712	10^+	$1.1^{+0.6}_{-0.5}$	$0.42^{+0.38}_{-0.15}$
576	12^+	$0.7^{+0.6}_{-0.5}$	$1.7^{+3.0}_{-0.8}$
561	14^+	$2.4^{+0.7}_{-2.2}$	$0.62^{+6.8}_{-0.14}$

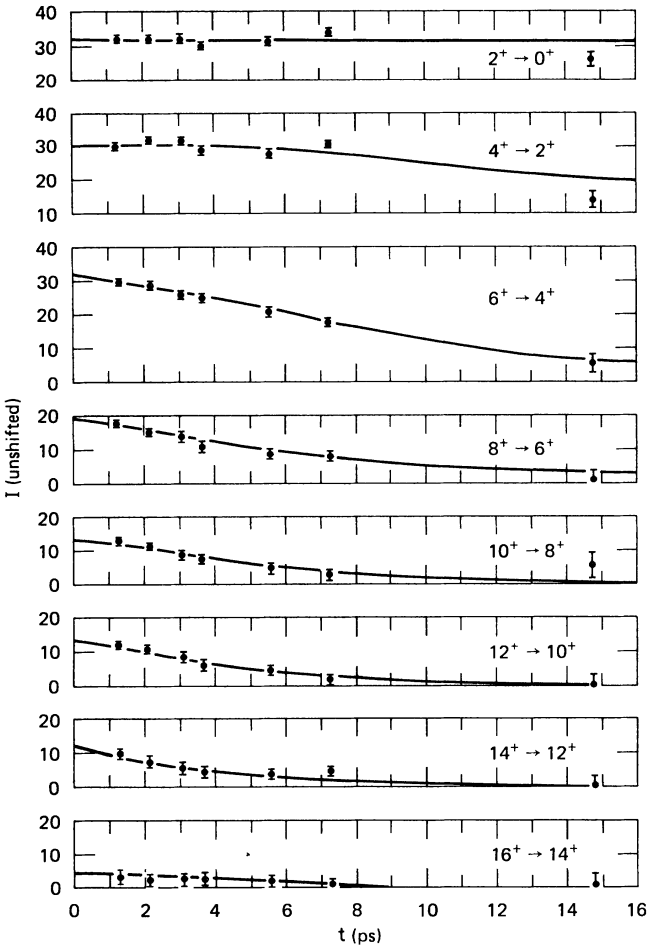

FIG. 5. Decay curves showing unshifted γ-ray intensities as a function of flight time for transitions in ^{128}Ce. The points represent the experimental data with application of the usual corrections described in the text. The solid curves are the fitted time distributions determined by the program LIFETIME (Ref. 7).

were fitted simultaneously, first with no feeding, then with one-step side feeding, and then with two-step side feeding. Next, starting with the highest level and working down, each level was fitted by itself with all other parameters fixed, then by varying its parameters plus those for all the levels above it. Finally, the levels were fitted in groups of three, and the lifetime of the center level of the group was adopted as the best value for that level.

Uncertainties on the lifetimes were determined by the method of the subroutine MINOS, described in Ref. 8. In this procedure, it is assumed that the point in the parameter space where χ^2 takes on its lowest value $\chi^2_{\min}$ determines the most likely or best-fit parameter values, and that the region over which χ^2 takes on values smaller than $\chi^2_{\min}+1$ corresponds to the "one-standard-deviation" confidence interval of 68%. The uncertainty for a given parameter was found by varying that parameter in steps above (below) its best value. At each step, it was fixed, and χ^2 was reminimized by varying all the other parameters. The step at which the reminimized χ^2 equaled $\chi^2_{\min}+1$ was used for the positive (negative) uncertainty for this parameter.

This procedure led to rather asymmetric error limits on some of the lifetimes and $B(E2)$ values. (See Tables I and II and Fig. 6.) The large upper limits on the $B(E2)$ values for the 12^+ and 14^+ states are due primarily to the unknown lifetimes of unseen side feeding, where 22% of the intensity of the 12^+ state, and 64% of that of the 14^+ state, was from side feeding. The fitting program could fit large transition rates for these states almost as well as the optimum ones by reducing the transition rates of the feeders appropriately. This problem was even more severe for the 8^+ state. Here, 40% of the intensity was from side feeding, of which 16% had a long (182 ps) lifetime.

Since the 16^+ state was the highest state for which we obtained a decay curve, we had no knowledge of the time distribution of the feeding intensity to it. When we used the two-step-cascade side-feeding model to this state, as was done with the others, we obtained a value for the lifetime of $5.8^{+4.3}_{-5.8}$ ps. When we used as a model the rotational band whose intrinsic quadrupole moment was a variable parameter, as already described, the lifetime value was 3.2 ± 1.0 ps. While we believe that there may be reasonable justification for using this latter model, we do not feel confident enough of this result to include it in Table I.

Uncertainties on parameters in least-squares fits are often determined by taking the square roots of the diagonal elements of the covariance matrix (the inverse of the matrix of second derivatives of χ^2 with respect to the parameters). This has the effect of looking at the curvature of the χ^2 function close to the minimum, and then extra-

TABLE II. $B(E2)_{\text{exp}}/B(E2)_{\text{rot}}$ for yrast transitions of light Ce isotopes.

	$B(E2)_{\text{exp}}/B(E2)_{\text{rot}}$ (normalized)						
	$2^+\rightarrow0^+$	$4^+\rightarrow2^+$	$6^+\rightarrow4^+$	$8^+\rightarrow6^+$	$10^+\rightarrow8^+$	$12^+\rightarrow10^+$	$14^+\rightarrow12^+$
^{128}Ce[a]	1.0	1.1 ± 0.2	$0.8^{+0.8}_{-0.3}$	$1.1^{+100}_{-0.5}$	$0.6^{+0.5}_{-0.2}$	$2.3^{+4.0}_{-1.1}$	$0.8^{+9.0}_{-0.2}$
^{130}Ce[b]	1.0	0.95 ± 0.10	0.54 ± 0.04	>0.7	0.52 ± 0.11	1.9 ± 0.4	1.9 ± 0.5
^{130}Ce[c]	1.0	$1.15^{+0.20}_{-0.13}$	$0.64^{+0.28}_{-0.17}$	>0.7	$0.50^{+0.53}_{-0.16}$	$0.59^{+0.16}_{-0.09}$	$1.8^{+3.0}_{-1.0}$
^{132}Ce[c]	1.0	$0.65^{+0.18}_{-0.13}$	$0.93^{+0.90}_{-0.34}$	>0.4	$0.14^{+0.04}_{-0.03}$	$\gtrsim1.6$	$0.70^{+0.20}_{-0.13}$
^{134}Ce[c]	1.0	$0.55^{+0.15}_{-0.10}$	$0.23^{+0.18}_{-0.08}$	>0.28	$0.0042^{+0.011}_{-0.006}$	$0.64^{+0.13}_{-0.08}$	$0.64^{+0.40}_{-0.18}$

[a]Present work.
[b]From Ref. 3.
[c]From Ref. 1.

polating up to χ^2+1, assuming the function is parabolic. If the χ^2 function is not parabolic, the errors obtained by the MINOS procedure will be different from these parabolic errors, often asymmetric and usually larger.

In our analysis, the MINOS uncertainty and the parabolic uncertainty were essentially the same for the lifetimes of the 2^+ and 4^+ states, but the MINOS uncertainties were considerably larger for those of the higher spin states. Had we quoted the parabolic errors, as is often done, our results would look better, but we have chosen to use the MINOS errors, which we believe give a more accurate assessment of the precision of the recoil-distance measurement.

IV. DISCUSSION

In Table II and Fig. 6 we show the ratios of experimental $B(E2)$ values to rotational $B(E2)$ values for yrast transitions in light cerium nuclei. For each nucleus, the rotational values were based on the $B(E2; 2^+ \rightarrow 0^+)$. It is seen in Fig. 6 that ^{130}Ce, ^{132}Ce, and ^{134}Ce exhibit a dropoff in $B(E2)$ strength at the backbending point, with the largest reduction in collectivity for the 10^+ state occurring in ^{134}Ce. In addition, ^{134}Ce shows a gradual dropoff for states below the backbend. Within experimental error limits, our ^{128}Ce data are compatible with rigid rotor $B(E2)$ values all the way through the 14^+ state. Beyond the backbend, all of these nuclei have $B(E2)$ values consistent with rotational predictions.

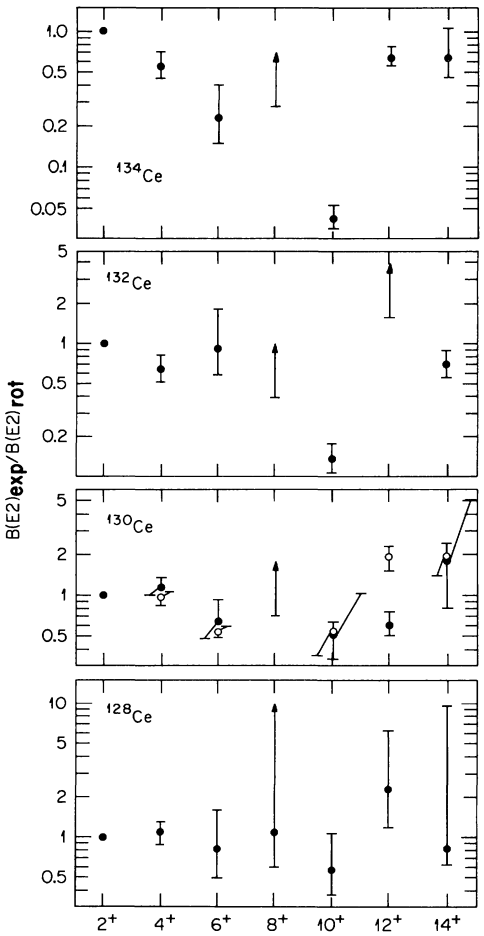

FIG. 6. Plot of $B(E2)_{exp}/B(E2)_{rot}$ of yrast transitions in ^{128,130,132,134}Ce nuclei.

The $B(E2)$ values in these light cerium nuclei suggest that a variety of regimes of theoretical description may be applicable between ^{134}Ce and ^{128}Ce. It is known[13] that ^{134}Ce behaves somewhat like a spherical nucleus with well-defined valence space. The decreasing trend of $B(E2)$ values for states up to 10^+ in ^{134}Ce are characteristic of the predictions of the seniority coupling scheme. On the other hand, the steady pattern of large collectivity observed in the present measurements for ^{128}Ce indicates that it is a rotational nucleus and, thus, has a reasonable basis for the application of a cranking-model analysis. It may be that the intermediate nuclei, ^{130}Ce and ^{132}Ce, are transitional in nature and can best be accounted for by the interacting-boson model and other models based on truncated, spherical configuration spaces. A reduction of the $B(E2)$ strength around the 10^+ states would, however, follow from all these models.

In ^{128}Ce, a strong backbend occurs at spin 10^+, just as is the case for ^{130}Ce, ^{132}Ce, and ^{134}Ce. A plot of the aligned angular momentum versus rotational frequency for these nuclei shows that they all have very similar crossing frequencies of ~ 0.3 MeV and have very similar values of the aligned angular momentum, viz., 8, 9, 10, and 9.3 for the sequence ^{128,130,132,134}Ce. Thus, it appears that the alignments all come from strongly decoupled high-j orbits, the $h_{11/2}$ protons, or the $h_{11/2}$ neutrons. Based on blocking measurements in ^{127}La and ^{129}La by Ward *et al.*[14] and in ^{131}Ce by Nolan *et al.*,[2] it is reasonable to assume that the $h_{11/2}$ protons give rise to the collectivity at the backbend in ^{128}Ce. However, as already alluded to, it appears quite probable that neutrons play a role in ^{134}Ce backbending, based on the measured g-factor value of -0.30 for the 10^+ state by Zemel *et al.*[13]

From the measured $B(E2)$ values for ^{128}Ce, it is possible to draw conclusions about the nuclear shape. Chen, Frauendorf, and Leander[15] have investigated the properties of quasiparticle orbits in the region of the light cerium nuclei. They carried out cranked shell-model calculations in which they were able to fit their parameters to the ^{130}Ce data of Nolan *et al.*[3] Their results show that the delicate balance between prolate-driving $h_{11/2}$ protons and oblate-driving $h_{11/2}$ neutrons in ^{128}Ce falls in favor of the prolate shape. In addition, Leander *et al.*[16,17] have carried out cranked self-consistent calculations for ^{128}Ce up to moderately high spin. Their calculations indicate that, for the yrast sequence, the quadrupole deformation parameter ϵ_2 remains essentially constant and that the asymmetry parameter γ does not leave the collective sector $-60° < \gamma < 0°$. This prediction holds for the ground band and the aligned bands for both $h_{11/2}$ protons and $h_{11/2}$ neutrons, in good agreement with our experimental data from spin 2 to 14.

ACKNOWLEDGMENTS

The authors wish to thank Georg Leander for his helpful discussions on this work and Hans Emling for supply-

ing us with the original version of the lifetime analysis program. We are also grateful to J. R. Tarrant, J. E. Weidley, and R. W. Miles for their help in various aspects of the design, construction, and testing of the recoil-distance device used here. This research was supported by the U. S. Department of Energy under Contract No. DE-AC05-84OR21400 with Martin Marietta Energy Systems, Inc.

---

*Permanent address: University of Jyväskylä, Jyväskylä, Finland.

†Permanent address: Australian National University, Canberra, Australia.

‡Permanent address: Texas A&M University, College Station, TX 77843.

[1]D. Husar, S. J. Mills, H. Gräf, U. Neumann, D. Pelte, and G. Seiler-Clark, Nucl. Phys. **A292**, 267 (1977).

[2]P. J. Nolan, D. M. Todd, P. J. Smith, D. J. G. Love, P. J. Twin, O. Andersen, J. D. Garrett, G. B. Hagemann, and B. Herskind, Phys. Lett. **108B**, 269 (1982).

[3]P. J. Nolan, R. Aryaeinejad, D. J. G. Love, A. H. Nelson, P. J. Smith, D. M. Todd, P. J. Twin, J. D. Garrett, G. B. Hagemann, and B. Herskind, in *Proceedings of the Conference on High Angular Momentum Properties of Nuclei, Oak Ridge, Tennessee, 1982,* edited by N. R. Johnson (Harwood-Academic, New York, 1983), p. 57; J. Phys. G (in press).

[4]J. L. S. Carvalho, Ph.D. thesis, Michigan State University, 1982 (unpublished).

[5]J. L. S. Carvalho, F. Bernthal, N. R. Johnson, I. Y. Lee, J. Hattula, L. L. Riedinger, and M. P. Fewell (unpublished).

[6]N. R. Johnson, J. W. Johnson, I. Y. Lee, J. E. Weidley, D. R. Haenni, and J. R. Tarrant, Oak Ridge National Laboratory Physics Division progress report ORNL-5787, 1981, p. 147.

[7]J. C. Wells, M. P. Fewell, and N. R. Johnson (unpublished).

[8]F. James and M. Roos, Comput. Phys. Commun. **10**, 343 (1975).

[9]N. R. Johnson, R. J. Sturm, E. Eichler, M. W. Guidry, G. D. O'Kelley, R. O. Sayer, D. C. Hensley, N. C. Singhal, and J. H. Hamilton, Phys. Rev. C **12**, 1927 (1975).

[10]R. J. Sturm and M. W. Guidry, Nucl. Instrum. Methods **138**, 345 (1976).

[11]D. Ward, H. R. Andrews, R. L. Graham, J. S. Geiger, and N. Rud, Nucl. Phys. **A234**, 94 (1974).

[12]S. W. Yates, N. R. Johnson, L. L. Riedinger, and A. C. Kahler, Phys. Rev. C **17**, 634 (1978).

[13]A. Zemel, C. Broude, E. Dafni, A. Geldberg, M. B. Goldberg, J. Gerber, G. J. Kumbartzki, and K. H. Speidel, Nucl. Phys. **A383**, 165 (1982).

[14]D. Ward, H. Bertschat, P. A. Butler, P. Colombani, R. M. Diamond, and F. S. Stephens, Phys. Lett. **56B**, 139 (1975).

[15]Y. S. Chen, S. Frauendorf, and G. A. Leander, Phys. Rev. C **28**, 2437 (1983).

[16]G. A. Leander, P. Arve, T. Bengtsson, I. Ragnarsson, and J. Y. Zhang, Nucl. Phys. **A400**, 97 (1983).

[17]G. A. Leander, S. Frauendorf, and F. R. May, in *Proceedings of the Conference on High Angular Momentum Properties of Nuclei, Oak Ridge, Tennessee, 1982,* edited by N. R. Johnson (Harwood-Academic, New York, 1983), p. 281.